Serbian Tribology Society

SERBIATRIB '23

18th International Conference on Tribology

Faculty of Engineering University of Kragujevac

Kragujevac, Serbia, 17 – 19 May 2023

APPLICATION OF THE FRACTAL GEOMETRY IN WEAR VOLUME CALCULATIONS AT MICRO SCALE

Nina BUSARAC[1], Nikola KOTORČEVIĆ[1], Slobodan MITROVIĆ[1], Dragan ADAMOVIĆ[1], Petar TODOROVIĆ[1], Nenad GRUJOVIĆ[1], Fatima ŽIVIĆ[1,*]

[1]Faculty of engineering, University of Kragujevac, Serbia

*Corresponding author: zivic@kg.ac.rs

Abstract: *This paper presents five different approaches in wear volume calculations when the contact loads are low, in micro scale. Experimental ball-on-flat tribological tests were realised, with flat samples of AlMg4.5Mn0.7 aluminium alloy in linear reciprocating contact with the ball made of aluminium oxide (Al_2O_3). Five different low loads were applied: 0.1 N, 0.25 N, 0.5 N, 0.75 N, and 1 N. Two methods of wear volume calculations can be considered as a common practice since they used geometrical approximation of the worn track, including optical images measurements and penetration depth parameter, as obtained by the nanotribometer. Three methods of wear volume calculations studied the possibility to use fractal theory. Fractal model wear was compared with wear volume calculated based on the wear track geometry. Results showed that fractal models are promising method in determination of the wear volumes under low loads. However further research is needed to define influential factors and how to define variables in the fractal model for the wear volume calculations.*

Keywords: *microwear, fractal model, fractal geometry, wear volume calculations, nanotribometer, penetration depth.*

1. INTRODUCTION

Determination of which wear mechanisms are present at a given tribomechanical system and quantification of that wear are generally challenging and still an active area of research [1]. Using measuring devices, it is possible to determine the amount of wear on the system elements, but not the contributions from adhesion, abrasion, surface fatigue, fretting or tribochemical wear mechanism. The process of friction or energy dissipation is identified by friction force and coefficient of friction, and the process of wear or mass dissipation is identified by wear parameters, which can be determined.

The process of wear without lubrication on the elements of tribomechanical systems develops as a consequence of the collapse of their contact layers [2]. When sliding on a clean unlubricated metal surface, ceramic or metallic counterbody locally wears the oxide film away, so direct contact can occur [3], causing asperities to cold weld together. Those junctions are then broken by the sliding force, producing wear debris, after which new bonds form, etc., therefore progressing the wear process, based on adhesion.

According to Archard law of adhesive wear, in conditions of sliding that are characterized by relatively low wear intensity and in the absence of lubricant, the wear volume V is proportional to

the sliding distance L and the external load F_N, and inversely proportional to the yield stress of the material of lower hardness σ_y, as shown in equation (1), where K represents the wear coefficient [2].

$$V = K\frac{F_N}{3\sigma_y}L \quad (1)$$

As research went further, the original Archard's formula got modified and more complex, so that it could take the randomness of the rough surface into consideration. To improve their calculations researchers resorted to fractal theory to model adhesive wear [4–6].

Besides adhesive wear, another relevant wear type for dry rough surface contact would be abrasive wear, which causes microcutting, microcracking and even microploughing in case of notable hardness difference between the elements in contact. Wu et al. [7] investigated dry sliding wear on aluminium alloys in different annealing states, with a steel ball counterbody and found abrasive wear to be a dominant mechanism at lower loads, transitioning into more adhesive dominant wear at higher loads. They also calculated wear volume using Archard's law.

Different methods have been used to determine the wear volume after tribological tests [8,9]:

- 3D profilometry or wear volume calculations based on topography of the wear profile determined by using optical images of the wear track, that considers: (i) entire wear track geometry, (ii) according to the ASTM G133 and (iii) ASTM D7755 standards,
- Gravimetry based wear volume calculations that cannot be reliably used for very small amounts of the worn material (e.g. nano or micro scales),
- Other methods of calculations that considers wear track geometry along the stroke length.

In general, the most common aspect of the wear volume determination is the image processing of the wear track. Depending on the applied method, results can be different, and especially large error can occur related to the irregularities of the shape of the wear track. Hence, researchers are studying advanced techniques for image processing that can overcome the issues of long time needed for the detailed profilometry or cross-sectional profiles collections and integration.

One of the powerful methods for image processing and pattern recognition is fractal geometry and fractal dimension techniques [10]. Fractal calculations can be efficiently used to describe very complex geometries and objects, as occurring in nature, including repetitive patterns, roughness variations, or texture. Fractal geometry is finding its application in many fields and accordingly it can be applied in wear volume calculations. There is a growing need for standard methods in determination of the wear volume under conditions of micro loads and very small amounts of worn materials.

This paper presents short pilot research related to the wear volume calculations under conditions of micro loads where wear volumes are very low. We used several methods for wear volume calculations, including a new approach that uses fractal geometry .

2. METHODS FOR WEAR VOLUME CALCULATIONS AT MICRO SCALE

2.1 Fractal theory for wear calculation

Fractal theory, in the context of tribological applications, is based on self-similarity or self-affinity of random rough surfaces. Self-similarity means that if a portion of the rough surface is divided into sub-pieces, those sub-pieces will be alike the original piece. Self-affinity is a related concept, but unlike self-similarity where scaling is the same in all directions, self-affine objects can have different scaling in all coordinate directions [10]. In our research, we used a novel wear calculation model (equation 2) developed for fractal rough surfaces [6] to quantify wear resulting from dry sliding friction between a wrought aluminium alloy surface and an aluminium oxide counterbody, and compared the results with more conventional methods of wear quantification.

In equation 2, a_r is the real contact area, μ is the friction coefficient, σ_s represents the yield

strength of the material subjected to wear, E is the equivalent elastic modulus of the pair (see equation 3), τ_b is the shear strength of the material subjected to wear, k_{we} and k_{wp} are elastic and plastic wear coefficients related to the topography of the contact surface, Ds is the two-dimensional fractal dimension (meaning fractal dimension reduced by one), G is the scaling factor, and ψ is the domain expansion factor (see equation 4).

$$V = \left(1 + \frac{{\sigma_s}^2}{{\tau_b}^2}\mu^2\right)^{\frac{1}{2}} \cdot a_r \cdot \left\{k_{we} + (k_{wp} - k_{we})\left[\frac{DsG^2\sigma_s}{(2-Ds)F_N} \cdot \left(\frac{\pi E^2}{225{\sigma_s}^2}\right)^{\frac{1}{Ds-1}}\right]^{\frac{2-Ds}{2}} \psi^{\frac{(Ds-2)^2}{4}}\right\} \cdot L \quad (2)$$

$$E = \left(\frac{1-{\nu_1}^2}{E_1} + \frac{1-{\nu_2}^2}{E_2}\right)^{-1} \quad (3)$$

In equation 3, ν_1 and ν_2 represent the Poisson's ratios of the triboelements, while E_1 and E_2 represent their elastic moduli.

$$\frac{\psi^{\frac{2-Ds}{2}} - \left(1 + \psi^{-\frac{Ds}{2}}\right)^{-\frac{2-Ds}{Ds}}}{\frac{2-Ds}{Ds}} = 1 \quad (4)$$

Real contact area a_r can be calculated as a ratio of external force and material strength – equation 5, or determined experimentally, using geometric parameters of the elements in contact and measuring the width of the wear track, which will be described in more detail in later section of this paper, on a ball-on-flat contact example.

$$a_r = \frac{F_N}{\sigma_y} \quad (5)$$

Strength limit σ_y is defined in equation 6.

$$\sigma_y = \sigma_s\left(1 + \frac{{\sigma_s}^2}{{\tau_b}^2}\mu^2\right)^{\frac{1}{2}} \quad (6)$$

There's an intuitive connection between fractals and surface roughness, and so a lot of research has been dedicated to describing the correlation between the fractal dimension and the surface roughness parameters [11–13]. Fractal dimension of a rough surface can be determined using developed methods such as the box counting method, covering method, blanket method, and many others [10, 14, 15].

2.2 Wear calculations based on geometrical features of the wear track

Besides the fractal geometry method, we used other methods based on conventional geometry. The first one, which we will refer to as 'the wear width method' determines volume of the wear track left on a flat sample by a ball counterbody, by measuring the wear width a. The second one, which we will refer to as 'the penetration depth method' also calculates the wear track volume, but using the penetration depth h as the measured parameter. Figure 1 illustrates an ideal wear track geometry, with parameters wear width a, penetration depth h, and track length L_s. Figure 2 shows wear width a, ball radius r, circle sector angle α and penetration depth h in a cross-sectional view.

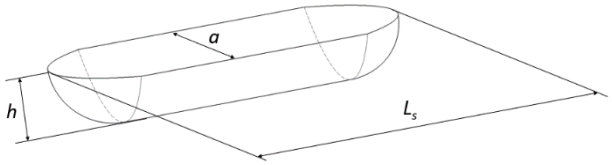

Figure 1. An ideal wear track geometry

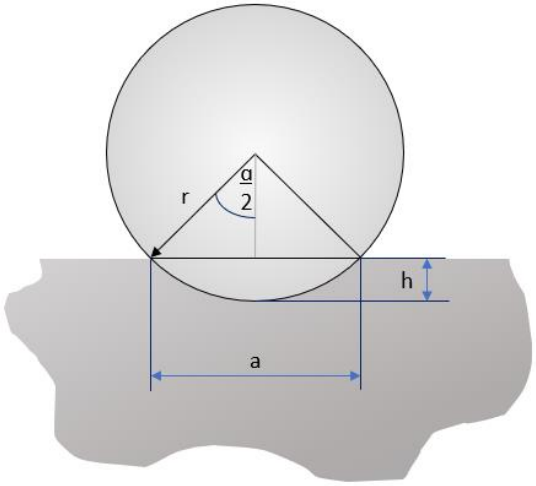

Figure 2. Relevant geometric parameters in cross-sectional view

If wear width is known (obtained by measuring), then circle sector angle can be calculated as shown in equation 7, and

penetration depth can be obtained as shown in equation 8.

$$\alpha = 2\sin^{-1}\left(\frac{a}{2r}\right) \quad (7)$$

$$h = r\left(1 - \cos\frac{\alpha}{2}\right) \quad (8)$$

On the other hand, if penetration depth is known, then circle sector angle can be calculated as shown in equation 9, and wear width can be obtained as shown in equation 10.

$$\alpha = 2\cos^{-1}\left(\frac{r-h}{r}\right) \quad (9)$$

$$a = 2r\sin\frac{\alpha}{2} \quad (10)$$

In any case, wear track volume is calculated using the equation 11, where V_o is spherical cap volume (equation 12) and P_o is circle segment area (equation 13).

$$V = 2\cdot\frac{1}{2}\cdot V_o + P_o\left(L_s - 2\cdot\frac{a}{2}\right) \quad (11)$$

$$V_o = \frac{\pi h^2}{3}(3r - h) \quad (12)$$

$$P_o = \frac{r^2\pi\alpha}{360} - \frac{a(r-h)}{2} \quad (13)$$

Contact surface area a_r (see equation 5) may be approximated using parameters in Figure 2, as shown in equation 14. The value will differ depending on approach – whether it is a wear width based or penetration depth based calculation.

$$a_r = 2\pi rh \quad (14)$$

3. MATERIALS AND METHODS

Square test samples (15x15 mm) were cut using waterjet technology from an aluminum alloy AlMg4.5Mn0.7 (EN AW 5083-H111) plate with the thickness of 4 mm. No additional surface treatment was done.

Flat sample of aluminum alloy AlMg4.5Mn0.7 was studied in contact with aluminum oxide (Al_2O_3) ball (1.5 mm diameter), at CSM nanotribometer (now Anton Paar) using reciprocating sliding motion. Test conditions were varied by using five values of the normal load: 0.1 N, 0.25 N, 0.5 N, 0.75 N, and 1 N. Sliding speed for all tests was 10 $^{mm}/_{s}$, and the amplitude of the linear reciprocating motion was 1 mm. All tests were repeated two times.

In the given tribomechanical system in which reciprocating sliding motion occurs, a ball of a higher hardness moves through the contact layer of the material of a lower hardness. At the same time, in the contact layer of the softer material, a compressive stress occurs in front of the ball, and a tensile stress occurs behind the hard ball, leading to the plastic flow of the material and debris formation, as illustrated in Figure 3.

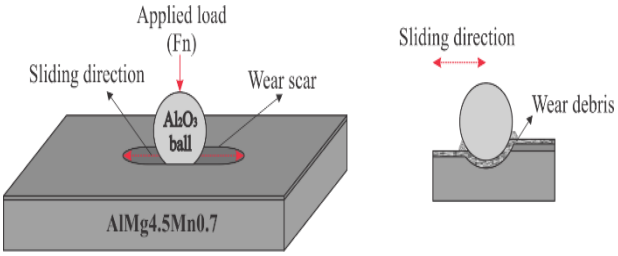

Figure 3. Sliding tribo-pair (not to scale)

After testing, relevant wear track dimensions such as wear width were measured using optical microscopy, and the penetration depth was acquired from the nanotribometer software, so that the volume of material lost could be calculated.

Surface roughness of aluminum samples was measured using a Taylor Hobson profilometer, and fractal dimension *D* was than estimated using fractal dimension roughness correlation [12], arriving at a value of 2.29.

Wear volume for each sample was calculated in five different ways.

Method 1: Wear volume was obtained from equation (11) and wear width via equation (10), by using experimental penetration depth (PD) parameter provided by the nanotribometer to calculate circle sector angle α as in equation (9) and equation (10).

Method 2: Wear volume was calculated from equation (11), where variable a (wear track width) was measured from optical images of the wear track. Equations (7) and (8) were used to calculate parameter h.

Method 3: Wear volume was calculated by using fractal theory and equation (2) and equation (5) for calculation of the parameter a_r, based on five different loads varied in experimental tests. Material characteristics for

aluminum alloy were taken from the literature. In this approach, normal load and alloy properties were included in equation (2).

Method 4: Wear volume was calculated by using fractal theory and equation (2) where parameter a_r was calculated via equations (14), (8) and (7), by using wear width (variable a) measured from the optical images.

Method 5: Wear volume was calculated by using fractal theory and equation (2) and parameter a_r was calculated via equation (14) and by using experimentally obtained PD values from nanotribometer software to calculate parameter h.

4. RESULTS

Graph representing wear volume results as a function of external load is given in Figure 4. All fractal model curves were fitted with a scaling factor of $G=1\cdot10^{-2}$, and wear coefficients of $k_{we}=1\cdot10^{-3}$ and $k_{wp}=6\cdot10^{-2}$.

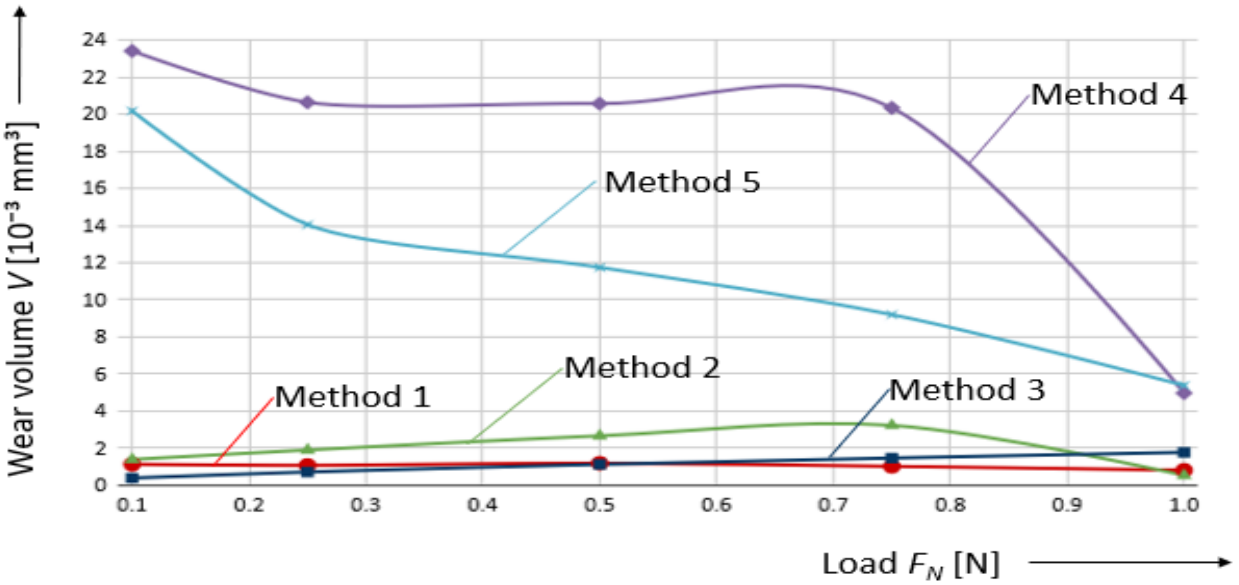

Figure 4. Wear volume V as a function of external load F_N; Method 1: using experimental penetration depth (PD) parameter; Method 2: measuring wear track width from optical images; Method 3: Fractal model where real contact area is approximated through normal load; Method 4: Fractal model where real contact area is approximated through wear track microscopy; Method 5: Fractal model where real contact area is approximated through experimental penetration depth (PD) parameter

It can be seen that wear volume curves in Figure 4 exhibit differences, based on the used method of calculation. Standard method that is commonly used is Method 2 by using measurements of the wear track width from optical images based on which geometrical approximation of the wear volume is calculated. Method 1 uses experimentally obtained penetration depth (PD) as provided by the nanotribometer software and it can be seen that differences occur for some load values (0.25 N, 0.5 N, 0.75 N). Fractal model applied to calculate wear volumes (Methods 3 – 5) shows large differences depending on the approach used in calculating real area of contact as previously shown. It is clear that Method 3 which only integrates applied normal load and material properties (yield strength and shear strength of the aluminium alloy) represents a good fit to the experimental methods (Method 1 and 2). However, fractal model with Methods 4 and 5 that additionally includes experimental measurements of either optical images of the wear track or penetration depth (PD) for the real contact area parameter a_r within equation (2) exhibits large differences compared to the standard Method 2, thus indicating that such approaches (Methods 4 and 5) are not valid.

5. DISCUSSION

During the testing of this tribomechanical system, alternating stressing of the contact layer of the softer material is repeated during a certain number of cycles, but the result cannot be accurately described as fretting or fretting

wear, as there is full rather than partial slip between elements [16] and no characteristic pits were observed.

After each test we noticed fine aluminum alloy particles adhered to the aluminum-oxide ball, suggesting the particles were trapped between the sliding elements, causing additional micro-level abrasive action, as the third body, rather than being indicative of galling.

Methods 1 – 3 produced rather similar results, while methods 4 and 5 differ in results due to the contact surface area approximation (equation 14) being greater than the real contact area, especially in the initial stages of the process, when contact is achieved only at a few asperities.

Comparing essentially similar methods 4 and 5, as well as methods 1 and 2, brings forward the discrepancy between wear width data acquired through microscopy and penetration depth data acquired from the tribometer. In both cases, calculations based on wear width give bigger wear volume values. This can be explained by two reasons, firstly, the actual wear track geometry is imperfect, unlike Figure 1, and optical measurements of the wear width are subjective to some degree, depending on the level of edge irregularities. Secondly, tribometer penetration depth measurements can be inexact due to debris collection between the sample and the counterbody – therefore penetration depth appears smaller.

Fractal theory could be used in estimation of the wear volumes, by using the normal load and material properties (yield strength and shear strength of the aluminium alloy). However, further research should indicate the best model fit of the fractal theory to comprise more test parameters into the model (e.g. wear track profilometry)

6. CONCLUSION

This paper presented five different ways of wear volume calculations. Optical images of the wear track commonly serve for the geometrical approximation of the worn material from the flat surfaces (Method 2 used in this article). We compared it with a method that uses penetration depth experimentally obtained from the nanotribometer (Method 1) and fractal model with three different ways of fitting the model to the wear volume calculations (Methods 3-5). We showed that fractal model cannot be used as a straightforward because it needs careful consideration. Fractal model as used in Methods 4 and 5 showed very large differences to the Method 2 that is used as a reference, thus indicating that these two approaches are not valid for the wear volume calculations. On the other hand, fractal model as used in Method 3 showed a very good fit with experimental Method 2.

Fractal mathematics for the studies of the rough surfaces has recently considerably progressed. Rendering real surfaces as fractals opens up new potential for material modeling and process quantification. Science is moving towards creating mathematical models that accurately capture the complex reality of real surface contact. However, to achieve more satisfactory results further research is needed.

ACKNOWLEDGEMENT

This paper is funded through the EIT's HEI Initiative SMART-2M project, supported by EIT RawMaterials, funded by the European Union.

REFERENCES

[1] P.M. Sieberg, S. Hanke: Challenges and Potentials in the Classification of Wear Mechanisms by Artificial Intelligence, Wear, 204725, 2023.

[2] B. Ivković, A. Rac: *Tribologija*, Jugoslovensko društvo za tribologiju, Mašinski fakultet, Kragujevac, 1995.

[3] B.N.J. Persson: *Sliding Friction: Physical Principles and Applications, Second edition*, Springer Berlin Heidelberg, Berlin, Heidelberg, 2000.

[4] W. Gong, Y. Chen, M. Li, R. Kang: Coupling fractal model for adhesive and three-body abrasive wear of AISI 1045 carbon steel spool valves, Wear, Vol. 418-419, pp. 75-85, 2019.

[5] X. Li, B. Wang: An Adhesive Wear Model Based on a Complete Contact Model for a Fractal

Surface, J. Phys. Conf. Ser., Vol. 2095, paper 012098, 2021.
[6] Z. Sha, Q. Hao, J. Yin, F. Ma, Y. Liu, S. Zhang: Wear calculation and life prediction model of disc brake based on elastoplastic contact mechanics, Adv. Mech. Eng., Vol. 14, No. 4, 2022.
[7] X. Wu, D. Wang, V. De Andrade, Y. Jiang, W. Wang, S. Wen, K. Gao, H. Huang, S. Chen, Z. Nie: Dry sliding wear of microalloyed Er-containing Al–10Sn–4Si–1Cu alloy, J. Mater. Res. Technol., Vol. 9, No. 6, pp. 14828-14840, 2020.
[8] M. Reichelt, B. Cappella: Comparative Analysis of Error Sources in the Determination of Wear Volumes of Oscillating Ball-on-Plane Tests, Front. Mech. Eng., Vol. 6, No. 25, 2020.
[9] J.J. Ayerdi, A. Aginagalde, I. Llavori, J. Bonse, D. Spaltmann, A. Zabala: Ball-on-flat linear reciprocating tests: Critical assessment of wear volume determination methods and suggested improvements for ASTM D7755 standard, Wear, Vol. 470–471, No. 203620, 2021.
[10] S.R. Nayak, J. Mishra, G. Palai: Analysing roughness of surface through fractal dimension: A review, Image and Vision Computing, Vol. 89, pp. 21-34, 2019.
[11] J.G. Ayala Landeros, V.M. Castaño Meneses, M.B. Becerra Rodríguez, S. Servín Guzmán, S.E. Román Flores, J.M. Olivare Ramírez: Correlation between Roughness (Ra) and Fractal Dimension (D) Using Artificial Vision Systems for On-Site Inspection, Comput. Sist., Vol. 22, No. 4, pp. 1473-1485, 2018.
[12] D. Chappard: Image analysis measurements of roughness by texture and fractal analysis correlate with contact profilometry, Biomaterials, Vol. 24, No. 8, pp. 1399-1407, 2003.
[13] X. Zuo, H. Zhu, Y. Zhou, J. Yang: Estimation of fractal dimension and surface roughness based on material characteristics and cutting conditions in the end milling of carbon steels, Proc. Inst. Mech. Eng. Part B J. Eng. Manuf., Vol. 231, No. 8, pp. 1423-1437, 2017.
[14] M. Wu, W. Wang, D. Shi, Z. Song, M. Li, Y. Luo: Improved box-counting methods to directly estimate the fractal dimension of a rough surface, Measurement, Vol. 177, No. 109303, 2021.
[15] X. Zhang, Y. Xu, R.L. Jackson: An analysis of generated fractal and measured rough surfaces in regards to their multi-scale structure and fractal dimension, Tribol. Int., Vol. 105, pp. 94-101, 2017.
[16] S. Fouvry, P. Arnaud, A. Mignot, P. Neubauer: Contact size, frequency and cyclic normal force effects on Ti–6Al–4V fretting wear processes: An approach combining friction power and contact oxygenation, Tribol. Int., Vol. 113, pp. 460-473, 2017.